

Probing the molecular connectivity of water confined in polymer hydrogels

B. Rossi, V. Venuti, A. Mele, C. Punta, L. Melone, V. Crupi, D. Majolino, F. Trotta, F. D'Amico, A. Gessini, and C. Masciovecchio

Citation: *The Journal of Chemical Physics* **142**, 014901 (2015); doi: 10.1063/1.4904946

View online: <http://dx.doi.org/10.1063/1.4904946>

View Table of Contents: <http://scitation.aip.org/content/aip/journal/jcp/142/1?ver=pdfcov>

Published by the [AIP Publishing](#)

Articles you may be interested in

[Structural changes of water in poly\(vinyl alcohol\) hydrogel during dehydration](#)

J. Chem. Phys. **140**, 044909 (2014); 10.1063/1.4862996

[Loading and release of internally self-assembled emulsions embedded in a magnetic hydrogel](#)

Appl. Phys. Lett. **104**, 043701 (2014); 10.1063/1.4862811

[Luminescence properties of Sm³⁺ doped YPO₄: Effect of solvent, heat-treatment, Ca²⁺/W⁶⁺-co-doping and its hyperthermia application](#)

AIP Advances **2**, 042184 (2012); 10.1063/1.4773443

[A controlled biochemical release device with embedded nanofluidic channels](#)

Appl. Phys. Lett. **100**, 153510 (2012); 10.1063/1.4704143

[Structural changes of water in a hydrogel during dehydration](#)

J. Chem. Phys. **130**, 034501 (2009); 10.1063/1.3058616



Probing the molecular connectivity of water confined in polymer hydrogels

B. Rossi,^{1,2,a)} V. Venuti,³ A. Mele,⁴ C. Punta,⁴ L. Melone,⁴ V. Crupi,¹ D. Majolino,¹ F. Trotta,⁵ F. D'Amico,¹ A. Gessini,¹ and C. Masciovecchio¹

¹*Eletra Sincrotrone Trieste, Strada Statale 14 km 163.5, Area Science Park, 34149 Trieste, Italy*

²*Department of Physics, University of Trento, Via Sommarive 14, Povo, Trento 38123, Italy*

³*Department of Physics and Earth Sciences, University of Messina, Viale Ferdinando Stagno D'Alcontres 31, 98166 Messina, Italy*

⁴*Department of Chemistry, Materials, and Chemical Engineering "G. Natta," Politecnico di Milano, Piazza L. da Vinci 32, 20133 Milano, Italy*

⁵*Department of Chemistry, University of Torino, Via Pietro Giuria 7, 10125 Torino, Italy*

(Received 8 September 2014; accepted 10 December 2014; published online 6 January 2015)

The molecular connectivity and the extent of hydrogen-bond patterns of water molecules confined in the polymer hydrogels, namely, cyclodextrin nanosponge hydrogels, are here investigated by using vibrational spectroscopy experiments. The proposed spectroscopic method exploits the combined analysis of the vibrational spectra of polymers hydrated with water and deuterated water, which allows us to separate and selectively investigate the temperature-evolution of the HOH bending mode of engaged water molecules and of the vibrational modes assigned to specific chemical groups of the polymer matrix involved in the physical interactions with water. As main results, we find a strong experimental evidence of a liquid-like behaviour of water molecules confined in the nano-cavities of hydrogel and we observe a characteristic destructuring effect on the hydrogen-bonds network of confined water induced by thermal motion. More interestingly, the extent of this temperature-disruptive effect is found to be selectively triggered by the cross-linking degree of the hydrogel matrix. These results give a more clear picture of the molecular mechanism of water confinement in the pores of nanosponge hydrogel and open the possibility to exploit the spectroscopic method here proposed as investigating tools for water-retaining soft materials. © 2015 AIP Publishing LLC. [<http://dx.doi.org/10.1063/1.4904946>]

I. INTRODUCTION

In recent years, a growing number of natural and synthetic polymer-based scaffolds have been implemented in most areas of regenerative medicine and tissue engineering in combined advanced technologies for replacing damaged or missing parts of living tissues.^{1–4} In particular, hydrogels have been proposed as efficient bio-compatible systems able to encapsulate cells or for local controlled drug delivery.^{5–7} Hydrogels obtained from cross-linked polymers after swelling with water solutions or biological fluids have been successfully implemented as carriers of bioactive macromolecules⁵ and for the controlled transport and release of drugs.^{6,7} In this sense, the geometry and dimension of the pores characterizing the polymeric network and the water-absorbing ability of hydrogels constitute key parameters for their efficient uses in targeted technological applications.^{8,9} Additionally, the study of water included in the hydrogels is a topic of relevance also for biological and technological implications, since the physical properties and state of the water confined in the polymer network can significantly affect the hydrogel stability and function.¹⁰

Cyclodextrin nanosponges (CDNS) are a promising novel class of nanoporous cross-linked polymers with pronounced properties of sorption of both organic and inorganic molecules.^{11–13} Several works are reported in recent literature that

exploit the performances of nanosponges as efficient nano-carriers for applications in agriculture,¹⁴ environmental control,¹⁵ and for pharmaceutical applications as drug stabilizers, bioavailability enhancers, and for drug delivery.^{16–18} CDNS can be easily synthesized by condensation reaction of the OH groups of the glucose units of cyclodextrins (CDs) with a poly-functional cross-linker agent (CL). For clarity, some typical examples of CL agents successfully used are activated derivative of a tetracarboxylic acid, like ethylenediaminetetraacetic acid dianhydride or pyromellitic anhydride (PMA) or a phosgene synthetic equivalent as carbonyldiimidazole. The synthesis leads to the formation of a statistic, three-dimensional network of cyclodextrin units, characterized by different types of cavities, namely, the apolar cavity of the CD macroring and the pores of the growing polymer. Their simultaneous presence in the structure of CDNS appears particularly beneficial for the capacity to encapsulate either lipophilic or hydrophilic active ingredients, protect them against undesired degradation, and enhance water solubility when necessary and thus increasing their bioavailability at the target site.¹⁷

Some types of CDNS showed a marked and selective swelling ability when contacted with water or water solution only, affording hydrogels.^{19,20} Indeed, the possibility to absorb, in a controlled way, a defined amount of water appears of particular practical importance in view of the possible use of CDNS as efficient water nano-containers²¹ and for an easy and efficient way to load the gel with a given compound (e.g., a pharmaceutical active ingredient) by swelling the

^{a)} Author to whom correspondence should be addressed. Electronic mail: rossi@science.unitn.it

polymer by an aqueous solution of the molecule of interest. In addition, CDNS-based hydrogels have been recently suggested to be good candidates as stimuli-responsive systems for entrapment/release of bio-active compounds, thanks to their ability to undergo modifications in their physical state (rigid gel network or liquid suspension) in a controlled way, by changing, for example, the hydration level of CDNS in water.^{20–24} Another aspect that makes CDNS hydrogels particularly attractive is the possibility of efficiently tuning specifically for applications the physical-chemical properties of CDNS by acting during the synthesis of polymers on some parameters, i.e., the chemical structure of CL and the relative amount of CL with respect to CD (n = molar ratio between cross-linking agent and CD). Among these factors, the molar ratio n was found to mainly influence the degree of reticulation of polymer matrix¹⁹ that is, in turn, strongly related to the dimension of cavities of CDNS and to their maximum water holder capacity.^{20,22–24}

In this scenario, it appears of paramount importance a deep understanding, at molecular level, of the state and properties of the water molecules confined inside the nano-cavities of CDNS in the gel state, in order to clarify the molecular connectivity of water located inside the nanosponge network and the extent of water-polymer interactions. Indeed, recent experimental results suggest that the complex relationship between chemical and physical forces established in the CDNS hydrogel over a mesoscopic length scale plays a crucial role in defining macroscopic properties of the systems, i.e., viscosity of the gel phase, its maximum water holding capacity,^{22–24} and diffusion behaviour of guest molecules inside the network.²⁵

Vibrational spectroscopy, especially if coupled with quantum chemical computation techniques, has been recognized as very useful tool for the structural elucidation of molecular systems and it has been recently successfully applied to the study of the complex polymeric network of cyclodextrin nanosponges.^{26–30} In the case of hydrated systems, vibrational spectra are particularly informative of the intra- and intermolecular modes of water molecules whose oscillator forces are sensitive, in turn, to the interactions with the solute or in general with their surroundings. In this sense, the inspection of Raman and infrared spectra of pure water and water-mixtures constitute an indirect way of studying the hydrogen bond (HB) intermolecular network of water molecules and their different levels of connectivity.^{31–35}

It is well known that confined water molecules, especially within the nano-scale cavities, exhibit physical properties and states (liquid or crystalline) different from those of bulk water. The different behaviour, in turn, depends on the molecular characteristics of the cavity surface, the confinement dimensions, temperature, and pressure.^{36–39} Generally speaking, it has been suggested that the water molecules confined in a nano-structured space are unable to form a long-range crystalline structure and thus the confined water remains liquid even below the ice crystallization temperature. Fourier Transform Infrared spectroscopy measurements have recently probed the existence of the low-density liquid phase in supercooled confined water by inspection of the temperature-evolution of the HOH bending and OH-stretching modes of water confined into nanopores.⁴⁰

In this paper, we discuss the temperature-evolution of the vibrational spectra of nanosponges hydrogel hydrated, in a combined way, with water and deuterated water. The behaviour of the HOH bending mode of water molecules engaged in the polymeric system is analyzed, in order to characterize the state and the dynamics of water molecules during the swelling process leading to the formation of the hydrogel. Interestingly, the spectroscopic data give evidence of the presence in the nano-cavities of nanosponges of water molecules that appear in liquid state even below the temperature of 270 K where usually the bulk water tends to crystallize.

In summary, the present work is aimed at the following goals: (i) to provide a rationale—at molecular level—of the mechanism of water confinement inside the pores of nanosponge hydrogel. The understanding of this phenomenon is a fundamental starting point for the modulation of the stability range of the liquid suspension and gel phases, also in view of the design of stimuli-responsive CDNS. (ii) To propose a spectroscopic method for probing the molecular connectivity and dynamics of water confined in polymer gels, such as hydrogel network, by using IR spectroscopy. Such methodology exploits the combined analysis of the vibrational spectra of polymers hydrated with water and heavy water in order to selectively investigate the spectral contribution directly associated to the solvent and to the polymeric matrix. The case example of cyclodextrin nanosponge hydrogel is chosen since CDNS are a good model system for the study of water-water and water-polymer interactions in hydrogel phases. Indeed, the structure of CDNS is characterized by the presence of both hydrogen-bond donor/acceptor groups and, additionally, some important parameters such as cross-linking degree, pore dimension, and hydrophilicity/hydrophobicity of the polymer matrix can be efficiently tuned by acting on the parameter, n .

II. EXPERIMENT

The nanosponges β -CDPMA1 n ($n = 4, 6, 8,$ and 10) were obtained by using β -cyclodextrin (β -CD) as monomeric unit and PMA as cross-linking agent. Following the synthetic procedure previously reported,^{11–13} anhydrous β -cyclodextrin (β -CD) was dissolved at room temperature in anhydrous DMSO containing anhydrous Et_3N . Then, the cross-linking agent PMA was added at 1: n molar ratios (with $n = 4, 6, 8,$ and 10) under intense magnetic stirring. The polymerization was complete in few minutes obtaining a solid that was broken up with a spatula and washed with acetone in a Soxhlet apparatus for 24 h. The pale yellow solid was finally dried under vacuum.

The corresponding hydrogel of CDNS was prepared by adding to the dry samples a suitable amount of double-distilled water (Sigma) in order to obtain the desired level, h , of hydration, i.e., $h = 0.4$. The hydration level, h , is defined as weight ratio of water/CDNS. The nanosponge hydrogels hydrated in deuterated water D_2O ($h = 0.4$) were prepared by following the same procedure. The gels were kept at room temperature during more than 12 h, before the Raman and IR measurements. No significant change in the spectrum was detected, indicating the full H/D-exchange between solvent and polymer.

FTIR-ATR absorption measurements were performed in the 400–4000 cm^{-1} spectral region for nanosponges hydrated both in H_2O and D_2O . The temperature range of 250 K–340 K was investigated. Spectra were recorded using a Bomem DA8 Fourier transform spectrometer, operating with a Globar source, in combination with a KBr beamsplitter and a thermoelectrically cooled deuterated triglycine sulphate (DTGS) detector. The samples of gel were contained in Golden Gate diamond ATR system, just based on the Attenuated Total Reflectance (ATR) technique. The spectra were recorded with a resolution of 4 cm^{-1} , automatically adding 100 repetitive scans in order to obtain a good signal-to-noise ratio and highly reproducible spectra. All the measurements were performed in a dry atmosphere. To check a possible unwanted effect induced by wetting and/or drying phenomena when the sample holder was filled with dry nitrogen, IR spectra in presence and absence of air were compared without showing any significant difference. All the spectra were normalized for taking into account the effective number of absorbers. No smoothing was done, and spectroscopic manipulations such as baseline adjustment and normalization were performed using the Spectralcalc software package GRAMS (Galactic Industries, Salem, NH, USA). The analysis of the 1500–1800 cm^{-1} region, that required a band decomposition procedure, was undertaken using the curve fitting routine provided in the PeakFit 4.0 software package.

UV Raman scattering measurements were carried out at the BL10.2-IUVS beamline at the Elettra Synchrotron laboratory in Trieste. The spectra were excited at 266 nm. Nanosponge hydrogels were directly prepared into the optical quartz cells and the polarized Raman spectra were collected in a back-scattered geometry by a triple stage spectrometer (Trivista, Princeton Instruments) with the spectral resolution of 1.0 cm^{-1} . To minimize potential photodecomposition of the gels resulting from UV laser exposure, the sample cell was subjected to slowly continuous spinning during the measurements in order to vary the illuminated sample volume through the laser beam. A complete detailed description of the experimental setup can be found elsewhere.⁴¹

III. RESULTS AND DISCUSSION

Figures 1(a) and 1(b) show the comparison between the Raman and infrared spectra of β -CDPMA14 nanosponge in the wavenumber range of 1500–1800 cm^{-1} , as an example. Both the spectra have been acquired on a sample of nanosponge in dry and hydrated states (black and cyan symbols in Fig. 1, respectively), in order to recognize and assign the vibrational modes of the polymer matrix in this specific spectral range before and after its hydration in water. For this purpose, the experimental profiles in Figs. 1(a) and 1(b) are compared with the theoretical Raman activity and infrared intensities, respectively. The calculated profiles have been obtained by quantum chemical computations performed on the molecular model of 1,2,4,5-tetracarboxybenzoic acid dimethyl ester.^{28,30} This model was built starting from the chemical structure of the cross-linking agent PMA and assuming that a maximum of two carbonyl groups of PMA can be simultaneously engaged

to form ester linkages with CD molecules. As previously reported,^{28,30} the model obtained in this way mimics with satisfactory accuracy the molecular environment of PMA after the reaction with the OH groups of cyclodextrins to form the ester bridges that constitute the polymer network of nanosponges. We remark that the experimental profiles of nanosponges and the theoretical vibrational spectra obtained for the model of bridging molecule can be easily compared in the wavenumber range of 1500–1800 cm^{-1} since in this spectral window cyclodextrins do not show any interfering vibrational band, both in the infrared and the Raman spectra.^{42,43}

On the basis of the wavenumber and relative intensities of the computed peaks, the experimental broad bands centred at about 1718 and 1720 cm^{-1} in Raman and infrared spectra of dry nanosponges, respectively, are associated to the stretching vibration modes of the carbonyl groups $\text{C}=\text{O}$ of the PMA residues. In particular, we can recognize in both Raman and IR spectra two different components, $\nu(\text{C}=\text{O})_{\text{ester}}$ and $\nu(\text{C}=\text{O})_{\text{carboxylic}}$, assigned to the stretching vibration of the $\text{C}=\text{O}$ belonging to the ester groups and to the carboxylic groups of PMA, respectively.²⁸ By inspection of the experimental Raman profiles in Fig. 1(a), two other components centred at about 1553 and 1604 cm^{-1} can be observed. These bands correspond to two distinct vibrations, labelled as $\nu(\text{C}=\text{C})_1$ and $\nu(\text{C}=\text{C})_2$, that mainly involve the stretching modes of the $\text{C}=\text{C}$ bonds of the aromatic ring of PMA. It is noteworthy that both $\nu(\text{C}=\text{C})_1$ and $\nu(\text{C}=\text{C})_2$ show a relative high Raman activity but they are practically IR-inactive, as deduced by the comparison with the theoretical vibrational spectra shown in Figs. 1(a) and 1(b). Additionally, the experimental IR profile in Fig. 2(b) exhibits a very intense broad band centred at about 1585 cm^{-1} , labelled as $\delta(\text{C}-\text{H})$, assigned to the bending modes of the $\text{C}-\text{H}$ groups of the aromatic ring of PMA residues.

The spectral modifications occurring in the Raman and IR profiles of CDNS after hydration of the polymer with water (hydration levels $h = 4$ and $h = 0.4$ for Raman and IR spectra, respectively) can be inspected in Figs. 1(a) and 1(b). The presence in the IR spectra of hydrated CDNS of an additional contribution at about 1640 cm^{-1} can be clearly observed in the spectrum of the hydrogel with respect to the vibrational bands found in the profile of the dry nanosponge (Fig. 1(b)). This contribution corresponds to the HOH bending mode of water molecules^{32,34,38,40} engaged in the system and it appears particularly intense in the IR spectra, even at low hydration levels ($h = 0.4$). Conversely, the comparison between the Raman spectra of dry and hydrated CDNS in Fig. 1(a) gives evidence that the contribution associated to the HOH bending mode of water exhibits a negligible intensity with respect to the signals associated to the vibration modes of CDNS polymer although the hydration level is 10 times greater than in the IR spectrum. This finding, together with the observation that the spectral region around 1600 cm^{-1} , where the HOH bending mode of water falls, is more free from interfering bands of polymer nanosponge in the IR spectrum with respect to the Raman profile suggests to focus the attention on the IR spectra for studying in detail the behaviour of HOH bending mode. At the same time, important information on the hydration-dependence of intensity of vibration modes associated to the chemical groups of water-swollen CDNS can be extracted by

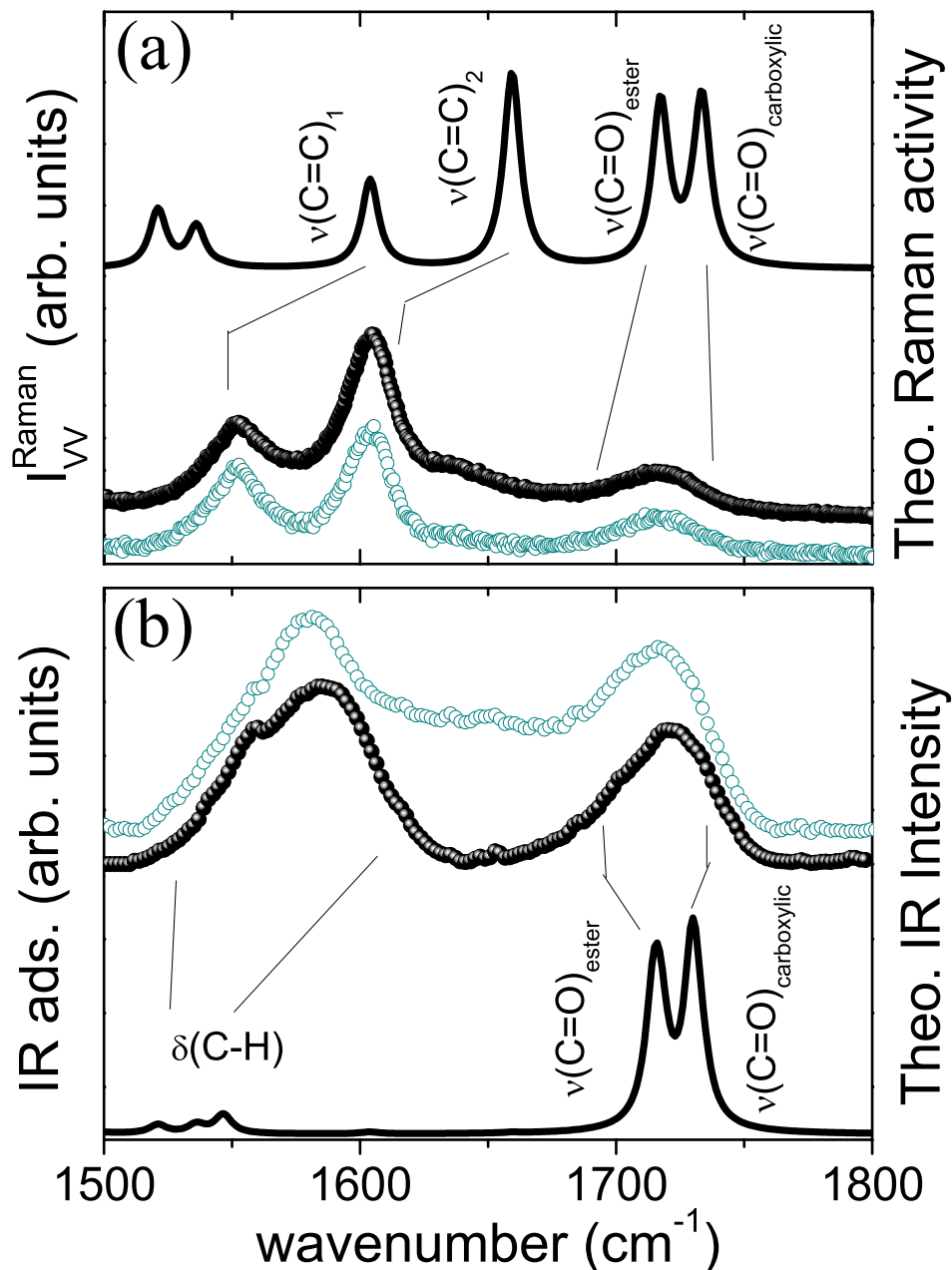


FIG. 1. Raman (a) and infrared (b) experimental intensities obtained for β -CDPMA14 nanosponge in dry (black symbols) and hydrated state (cyan symbols) compared with the corresponding theoretical Raman activity and infrared intensity (continuous line) obtained for the simulated model of 1,2,4,5-tetracarboxybenzoic acid dimethyl ester.^{28,30}

detailed inspection of Raman spectra and will be reported elsewhere.

The temperature-evolution of the IR spectra recorded on a sample of β -CDPMA14 after hydration with water (hydration level $h = 0.4$) are displayed in Fig. 2(a) in the spectral window $1500\text{--}1800\text{ cm}^{-1}$ and at different selected temperatures. Fig. 2(b) shows the IR spectra acquired on β -CDPMA14 hydrated with D_2O at the $h = 0.4$ and at the same temperatures of the data reported in Fig. 2(a). It appears evident that in the spectra of hydrogel prepared with deuterated water the characteristic HOH bending mode of engaged H_2O is not present, as expected. Indeed, it is well known²⁰ that the DOD (deuterium-oxygen-deuterium) bending mode of D_2O is shifted in the vibrational spectra to 1210 cm^{-1} . Thus, the use of D_2O instead of H_2O for the polymer swelling

allows us to separate and to examine the effect of the water confinement on the vibration modes assigned to the hydrogel matrix and on the HOH bending mode of engaged H_2O molecules.

The experimental profiles of Fig. 2 point out that the increase of temperature is responsible for considerable variations of the IR spectrum of the hydrogel. The feature at about 1640 cm^{-1} associated to the HOH bending mode of H_2O tends to become more intense at high temperatures and, at the same time, the total intensity of the $\delta(\text{C}-\text{H})$ and of the $\text{C}=\text{O}$ stretching band of the polymer decreases. The temperature-evolution of the vibrational modes of nanosponge can be better visualized looking at the profiles of Fig. 2(b), where these bands are not strongly deconvoluted with the bending mode of water.

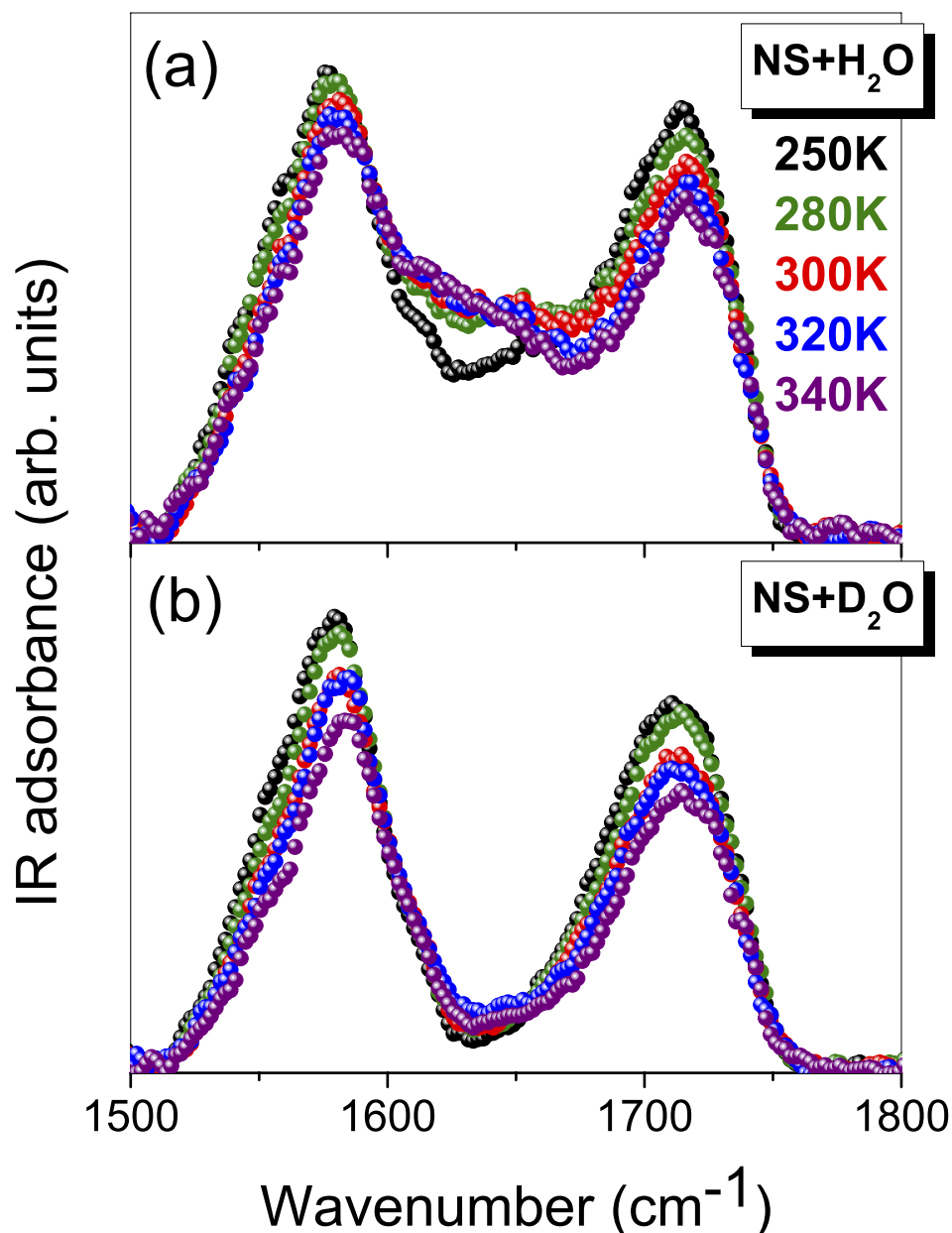


FIG. 2. Temperature-evolution of the infrared spectra obtained for β -CDPMA14 nanosponge hydrated in H_2O (a) and D_2O (b).

The decreasing intensity of the $\text{C}=\text{O}$ stretching mode in PMA-nanosponge hydrogel as a function of temperature is consistent with previous experimental investigations^{20,44} and it has been explained by taking into account that the thermal motion tends to induce a destructuring effect on the hydrogen bond network of H_2O or D_2O molecules which surround the $\text{C}=\text{O}$ groups of the polymer. As a consequence, the electrostatic environment experienced by these chemical groups of polymer is such that it reduces the overall dipole moment of the CO functional group.²⁰ Interestingly, the observed decreasing intensity of the $\delta(\text{C}-\text{H})$ mode of nanosponge suggests that also the CH groups of the aromatic ring of PMA are strongly involved in non-conventional hydrogen bonds interactions with water molecules of the type $\text{C}-\text{H}\cdots\text{O}-\text{H}$. The hydrogen bond donor character of the CH fragment in PMA is activated by both the sp^2 hybridization of the C atom and the aromatic frame in which the CH moiety is inserted.

In order to better emphasize the temperature-behaviour of the HOH bending mode of confined water, we report in Figure 3 the spectral contribution of this mode at two different temperatures. Such mode is isolated by considering the experimental profiles of β -CDPMA14 hydrated in H_2O and in D_2O . The profile in deuterated water is then subtracted from the corresponding in H_2O . The spectra in H_2O and D_2O have been preliminary normalized to the intensity of the band at about 1030 cm^{-1} , assumed as a reliable internal standard.^{20,27,28,30} Indeed, the latter vibrational mode is related to stretching vibrations of $\text{C}-\text{O}$ groups of cyclodextrin molecules that are not expected to be affected by the hydration of the nanosponge or by a variation of temperature.

Figure 3 presents the superimposition of the normalized spectral profiles of the protium and deuterated hydrogels in the spectral region, $1500\text{--}1800\text{ cm}^{-1}$. The profiles of D_2O hydrogels trace, within the experimental error, the corresponding

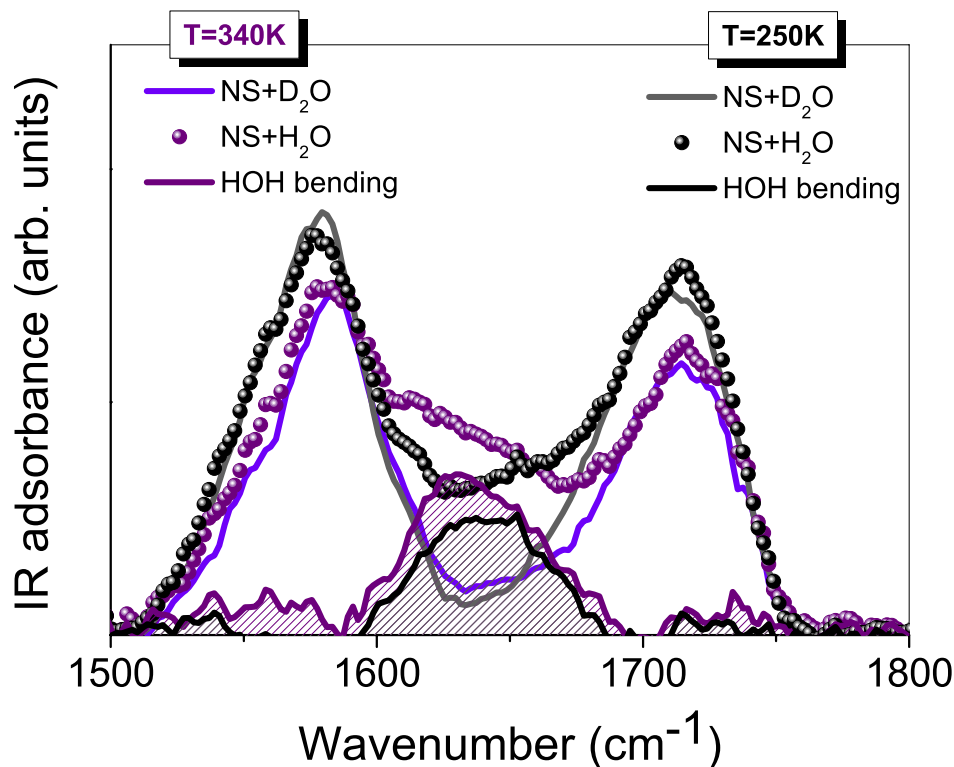


FIG. 3. Infrared spectra obtained for β -CDPMA14 nanosponge hydrogel (solid circles) at $T = 250$ K and $T = 340$ K; in the same panel, the contribution of HOH bending of water was isolated by subtraction of the signal of nanosponge hydrogel in D_2O (see text for details).

spectra in H_2O except for the component of HOH bending mode. This finding confirms the reliability of the data handling followed for the subtraction of the spectra.

As first important result, we find that HOH bending mode of water at $T = 250$ K (Fig. 3, full black line) shows a characteristic Gaussian-like form different from the nearly flattened profile typically exhibited by polycrystalline ice at the same temperature.^{34,40,45} Indeed, previous IR measurements independently performed by different authors,^{34,40,45} consistently show that during the phase transition, the IR absorption band of the bending mode of water undergoes sharp changes in the spectra of both H_2O and D_2O : In the solid phase, the bending mode appears very weak, while in the liquid state this band is a dominating peak. Moreover, in the crystalline ice at temperatures below of $T = 264$ K, the HOH bending mode rapidly vanishes and it appears as a very weak flattened profile, as clearly shown in Refs. 34 and 45. Based on these considerations, the spectra of Fig. 3 give evidence that the H_2O molecules engaged in the polymer network of nanosponge remain in liquid state even below the nucleation temperature where usually the bulk water crystallizes. This finding, recalling what already observed for water entrapped in a variety of amorphous porous materials and phyllosilicates,^{40,46–48} is consistent with the conclusion that water is strongly confined in the nano-cavities of nanosponge polymer in the hydrogel phase.

In addition, the comparison of the HOH bending mode observed at $T = 250$ and 340 K (Fig. 3) points out an increase in intensity of this mode and a slight shift to lower wavenumber upon the increase of temperature. This behaviour, recalling what already observed in bulk water^{32–34} and in water

confined in other nano-porous systems,^{40,46–48} indicates a sudden decrease in the molecular connectivity of the water molecules arranged in hydrogen bond networks as a consequence of the thermal motion.

In order to better quantify the temperature-effects on the HOH bending mode observed on the raw experimental data, the IR spectra of H_2O -hydrogel were fitted by using five Voigt functions for reproducing the vibrational bands of nanosponge matrix^{28,30} and one single Voigt curve for modelling the HOH bending mode of water.

The fitting curve obtained by following this procedure for the spectra of β -CDPMA14 nanosponge hydrogel in H_2O at $T = 290$ K is reported in Figure 4, together with the six distinct contributions of pure CDNS and HOH bending of water. The residual, also reported in the same Fig. 4, shows a negligible extra contribution in all the spectra region of interest, giving evidence of the reliability of the decomposition procedure. It is noteworthy that, in order to reduce the number of free fitting parameters in the analysis of profile of Fig. 4, the centre-frequencies of the components associated to the CDNS modes have been fixed to the values obtained by a preliminary fit of the corresponding D_2O -hydrogel spectrum, which is well reproduced as a sum of five Voigt contributions (see inset of Fig. 4).

In Figure 5, we report the spectral components associated to the HOH bending mode of water as obtained by fitting of experimental IR profiles of H_2O -hydrogel at different values of temperature.

The evolution of the curves better emphasizes the trend already observed on raw data (Fig. 3), consisting of a progressive shift towards lower wavenumber and a simultaneous

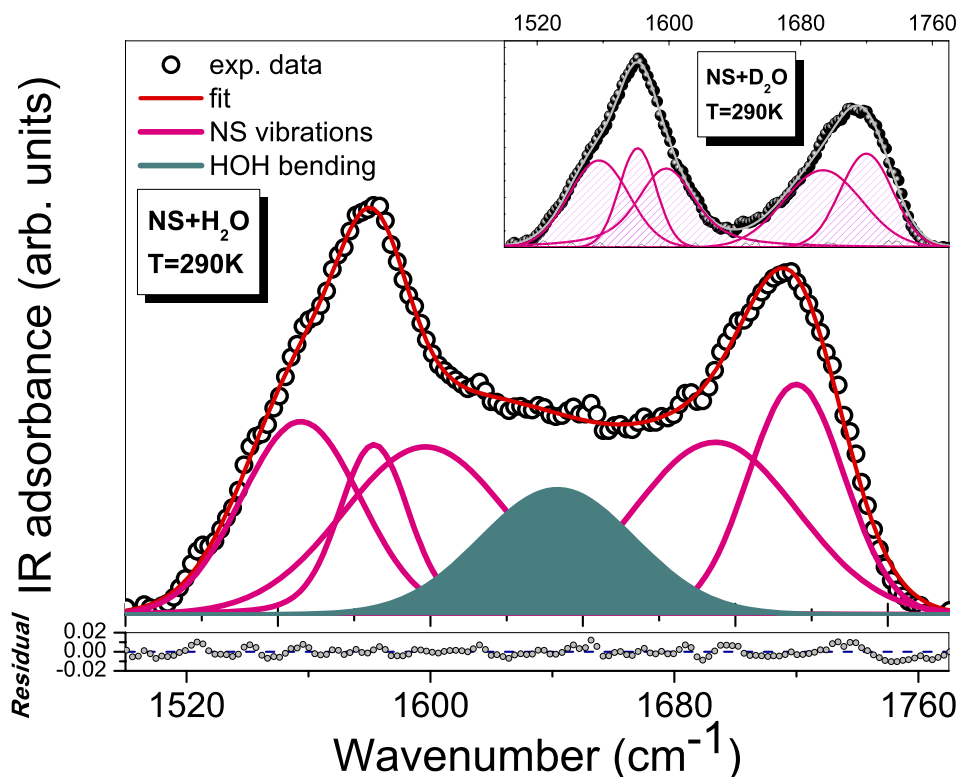


FIG. 4. Infrared spectra of β -CDPMA14 nanosponge hydrogel in H_2O at $T = 290$ K; the total fit curve (red line) is shown together with the single component; vibrations of pure NS (pink) and HOH bending of water (cyan full line). Inset: best-fitting results for β -CDPMA14 nanosponge hydrogel in D_2O at $T = 290$ K.

increase in intensity of the HOH bending mode of engaged H_2O upon the increase of temperature. This temperature behaviour is consistent with the evolution observed for the HOH bending mode in bulk water, as widely reported and discussed in literature^{31–34,45} by different authors. The experi-

mental IR spectra of bulk water acquired in the temperature range between 264 and 320 K^{34,45} show that, unlike the OH stretching band, the HOH bending mode decreases in intensity upon cooling and almost vanishes at the crystallization. Moreover, as the temperature is lowered, the position of its

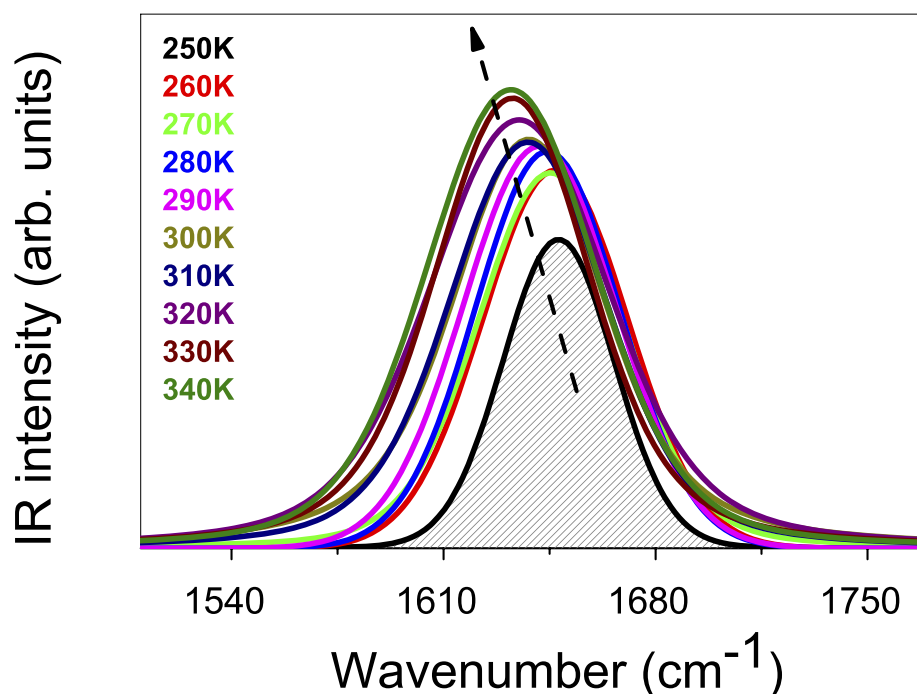


FIG. 5. Temperature-evolution of the HOH bending mode of water as estimated by fitting of experimental IR spectra of β -CDPMA14 nanosponge hydrogel (see text for details). The arrow indicates the increase of temperature.

maximum shifts towards higher wavenumber.³⁴ The behaviour observed for HOH bending mode in bulk water suggests the interpretation that the bending band mostly reflects the population of water molecules that do not lie in a symmetric tetrahedral environment,³⁴ giving indication the HOH bending mode is hardly sensitive to the different levels of connectivity of HB patterns developed by H₂O.

The curves shown in Fig. 5 indicate that as T increases the water molecules confined in the pores of nanosponges tend to reduce their level of molecular connectivity, similar to what happens in bulk water at high temperatures^{31–34,45} and recalling the behaviour observed for water entrapped in a variety of porous materials and phyllosilicates.^{40,46–48} The spectral modifications displayed in Fig. 5 can be interpreted taking into account that the thermal motion, enhanced by increasing temperature, tends to break the tetrahedral arrangements of water molecules favouring the re-organization of confined H₂O in not fully HB patterns. As mentioned above, it is noteworthy that the intensity of HOH bending mode of water confined in nanosponges remains relatively high even at temperatures below the crystallization temperature (see profile at T = 250 K in Fig. 5) different from what occurs in bulk water.^{34,45} This occurrence suggests that the water molecules confined in the pores of CDNS develop, even at temperatures below crystallization, transient HB arrangements with a mean coordination number less than four.

Although the destructuring effect on the HB network of H₂O engaged in CDNS, observed upon the increase of temperature, is in a way expected, interestingly it seems to be strongly affected by the specific features of the polymeric network of nanosponges. In Figure 6, the temperature-evolution of the wavenumber position ω_{HOH} of the HOH bending mode of water, estimated by the fitting procedure

described above, is shown for hydrogels obtained from different types of nanosponges β -CDPMA1n (n = 4, 6, 8, and 10, each at hydration level h = 0.4). We use the value of ω_{HOH} as a parameter for a quantitative evaluation of the destructuring effect, since it is reasonably considered more reliable with respect to the intensity of the HOH bending mode.

The data in Fig. 6 seem to suggest a linear dependence on T of the ω_{HOH} for all the types of nanosponge-hydrogel examined but with a different slope. Interestingly, the maximum slope is obtained in the case of β -CDPMA16 nanosponge hydrogel. In addition, we observe that for the latter type of hydrogel the HOH bending mode of water is more and more shifted towards the low wavenumber with respect to the other hydrogels at all the examined temperatures. The inset of Fig. 6 shows, as an example, the position ω_{HOH} as a function of the molar ratio n, at T = 300 K (n is the relative amount of cross-linking agent with respect to the monomeric unit cyclodextrin used in the synthetic protocol of preparation of nanosponges^{26,28}). This graph displays a triggering of the population of the non-tetrahedrally coordinated water molecules in correspondence with a 6-fold excess of cross-linker with respect to CD, closely recalling what has been systematically observed for other micro- and macroscopic properties of nanosponge hydrogel, such as stiffness,^{26,29} cross-linking density,²⁸ and absorption ability.^{22–24}

The data reported in Fig. 6 indicate that, in the explored T range, the hydrogen bonded network established among the water molecules confined in the nano-cavities of nanosponge hydrogel tends to be maximally destroyed when H₂O is adsorbed by β -CDPMA16 polymer. Conversely, high values of the parameter, n, in β -CDPMA1n polymers tend to favour the rearrangement of engaged water molecules in highly coordinated tetrahedral networks. This result is fully consistent

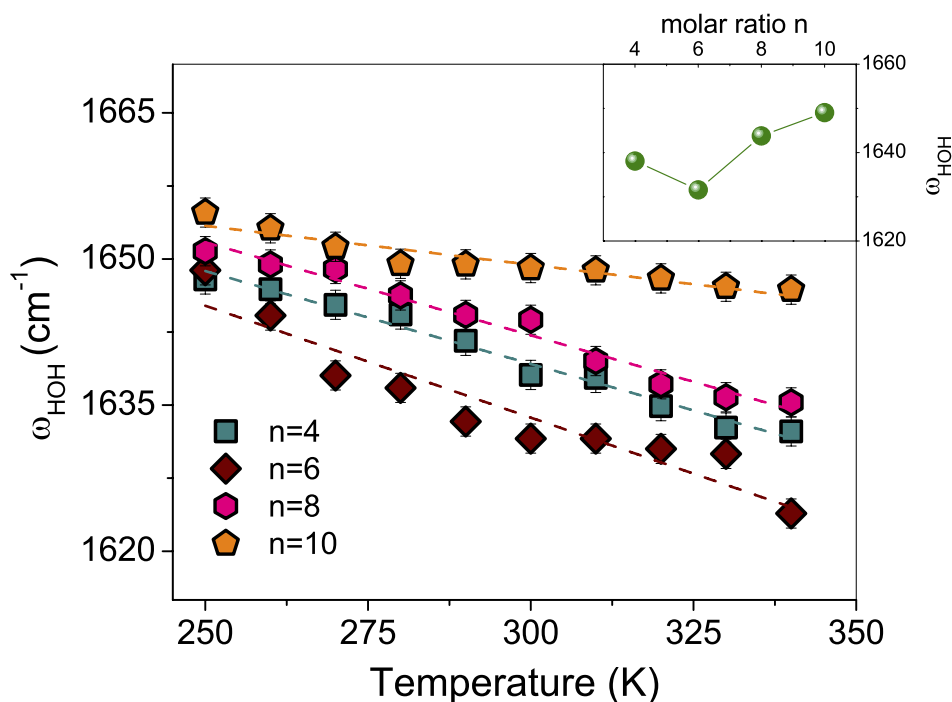


FIG. 6. Estimated position ω_{HOH} of HOH bending mode of water as a function of temperature for β -CDPMA1n nanosponge hydrogel (n = 4, 6, 8, and 10). Inset: position ω_{HOH} as a function of molar ratio n, at T = 300 K.

with previous investigations,^{20,24} and it can be explained by using a simple model that describes the n -dependence of the cross-linking process of cyclodextrins to form nanosponge.⁴⁹

It has been demonstrated that for molar excess less than a six-fold excess ($n = 6$) the cross-linking process is dominating. This critical value seems to be the result of an ideal balance between activated carboxylic groups and free hydroxyl functions onto the CD units, leading to the highest interconnectivity between the monomers. Conversely, larger excess of cross-linker ($n > 6$), causes branching of CD units rather than increasing the cross-linking degree, as also probed by experimental previous results.^{26,29,30} Then, we can conclude that the maximum cross-linking density of polymer network obtained at $n = 6$ tends to amplify the disruptive effect caused by the thermal motion on the confined water molecules. This occurrence is, in turn, to be ascribed to the fact that β -CDPMA16 nanosponge may have pores of smaller dimensions with respect to the other samples, as β -CDPMA16 exhibits the highest cross-linking degree. The latter hypothesis seems to be confirmed by small angle neutron scattering measurements recently performed on the CDNS hydrogel which will be reported elsewhere.

The n -dependence of hydrogen-bond connectivity in the water molecules confined in CDNS hydrogels, as pointed out in the inset of Fig. 6, can be correlated with the evolution, as function of n , of the C=O stretching band of β -CDPMA16 nanosponge²⁰ in gel phase. Previous IR and Raman measurements revealed that the hydration of nanosponges leads to the establishment of a HB network involving the C=O functional groups of the polymers, whose connectivity pattern is strongly dependent on the parameter, n . In particular, the marked shift to lower frequency observed for the C=O stretching band of β -CDPMA16 hydrogel with respect to the other samples²⁰ suggests that at molar ratio $n = 6$ corresponds to the establishment of the most strongly interconnected HB network involving the C=O groups of polymer. On the other side, higher values of n were found to induce destructuring effects on the HB interactions established among C=O moieties, probably due to the increased steric hindrance of the polymeric network introduced by the excess of cross-linker.

All these experimental results can be interpreted in light of a comprehensive model taking into account the different HB interactions which can be established in the gel phase, i.e., polymer-polymer, water-polymer, and water-water HB interactions. On one side, the maximum amount of crosslinking observed in dry PMA-nanosponges at a 6-fold excess of PMA with respect to β -CD is also consistent with the formation, in the hydrogel, of the most strongly interconnected HB network among the C=O groups of CDNS, at the expense of the population of water molecules arranged in tetrahedral HB networks. Otherwise, for $n > 6$, the addition of cross-linker increases the branching of CD units⁴⁹ and introduces some destructuring effects, mainly of entropic nature, that are responsible for the decrease of connectivity in the HB network established among C=O groups of polymers. This occurrence, in turn, favours the reorganization of confined water molecules in more interconnected tetrahedral HB arrangements.

Finally, we discuss, as example, the temperature-evolution of the IR spectra of β -CDPMA14 hydrated in D₂O in the high-

frequency range of 2700–3700 cm⁻¹ (Figure 7, panel at the top), where the characteristic OH stretching modes (ν_{OH}) of water are typically observed.^{20,22–24,44}

As suggested by other authors in the case of aqueous solutions of proteins,⁵⁰ the use of D₂O as solvent allows to selectively probe the ν_{OH} modes of water molecules resulting from isotopic exchanges between the superficial H atoms of CDNS and the solvent D₂O placed closely around the polymer surface, namely, DHO (deuterium-hydrogen-oxygen) water molecules. These water molecules give a contribution to the IR spectrum in the OH stretching region between 2700 and 3700 cm⁻¹ which appears significantly different from that observed in H₂O, as pointed out in the inset of Fig. 7. This occurrence, in agreement with previous studies,^{51–53} is consistent with the hypothesis that the DHO spectrum reflects a population of water molecules which more strongly interact with the chemical groups of CDNS within the nano-cavities of the polymer in hydrogel. Consequently, the DHO spectrum can be considered to be free of intermolecular coupling vibrations and it is called uncoupled stretching region.⁵⁰

As a general trend, we observe a significant shift to higher frequency of the DHO spectrum upon the increase of temperature (Fig. 7, panel at the top) together with an attenuation in intensity of the low-frequency contributions of the DHO stretching band (shoulder at about 3250 cm⁻¹). As expected, a similar trend is found also for the OH stretching band of engaged water, as evident by inspection of the spectra of β -CDPMA14 hydrogel in H₂O at two different temperatures (Fig. 7, panel at the bottom). These experimental findings are consistent with the behaviour observed and above discussed for the HOH bending mode of water and confirm the destructuring effect induced by the thermal motion on the water molecules confined in nanosponge hydrogel.

As widely reported in literature,^{51,54–56} the ν_{OH} vibrations of water are particularly sensitive to the co-operativity of the HB arrangements developed by the solvent molecules in the hydrogel. This suggests that the DHO spectrum may be interpreted in terms of the local environment of the water molecules present in the system.^{51,54–60}

By recalling a well assessed model^{57–60} already applied to the analysis of the OH stretching band in Raman and IR spectra of CDNS hydrogel,^{20,22–24,44} the spectral modifications observed in the DHO spectrum can be quantitatively related to different co-operativity degrees of the HB arrangements of water more closely confined in the pores of CDNS polymer. After a preliminary subtraction from the total DHO profile of the spectral signal assigned to the CH vibrational modes of nanosponges (signals falling between about 2760 and 3050 cm⁻¹), the DHO stretching band of water has been decomposed into four different contributions corresponding to four classes of OH oscillators present in the system.^{57–60} A typical result of the fitting procedure obtained for the DHO spectrum of β -CDPMA14 nanosponge hydrogel at $T = 300$ K is shown in Fig. 8 (panel at the top).

Taking into account the interpretation of the spectral components of the OH band as reported in literature,^{57–60} the sum of the percentage intensities of the two sub-bands at the lowest wavenumbers, labelled as $I_1 + I_2$, can be used to describe the population of water molecules arranged in tetrahedral HB

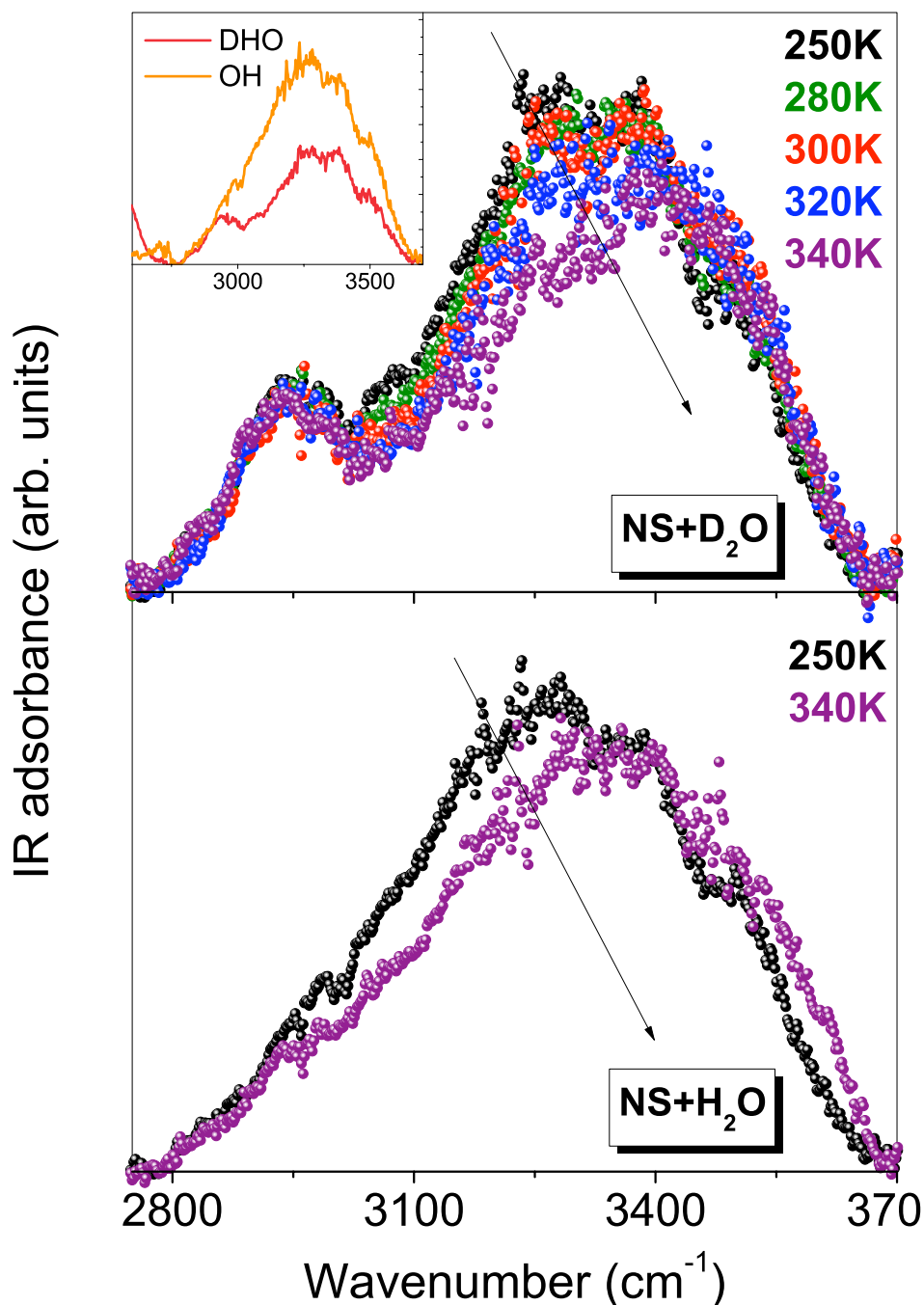


FIG. 7. Selected IR spectra of β -CDPMA14 nanosponge hydrogel in D_2O (panel at the top) and H_2O (panel at the bottom) at different values of temperature in the high-frequency range of $2700\text{--}3700\text{ cm}^{-1}$. The arrows in the panels indicate the increase of temperature. Inset: comparison between the OH stretching band in H_2O -gel and in DHO spectrum, at $T = 250\text{ K}$.

networks that exhibit strong hydrogen bonding on both the hydrogen atoms. Conversely, the sum of the two other contribution to the DHO band, $I_3 + I_4$, is representative of the population of water molecules that develop less strongly interconnected HB patterns with coordination number less than four.^{22–24}

The temperature-dependence of percentage intensities $I_1 + I_2$ and $I_3 + I_4$ obtained for the DHO spectrum is reported in the panel at the bottom of Fig. 8. It clearly appears that an increase of the temperature, T , corresponds to a reduction of the population of water molecules arranged in tetrahedral HB networks ($I_1 + I_2$), i.e., bulk-like contribution. Correspondingly, an enhancement of the population of water molecules involved

in HB network with connectivity less than four ($I_3 + I_4$, not bulk-like water) is observed upon the increase of temperature. The plot of Fig. 8 shows the existence of a characteristic crossover point at about $T = 280\text{ K}$, where the population of not bulk-like water molecules becomes favoured with respect to the population of bulk-like water.

A similar temperature-behaviour is found also for the percentage intensities of the spectral contributions to the OH stretching band of water (Fig. 8, at the bottom), as obtained by fitting and decomposition procedure applied to the spectra of hydrogel in H_2O . However, in the case of OH band, the characteristic crossover temperature where the population of

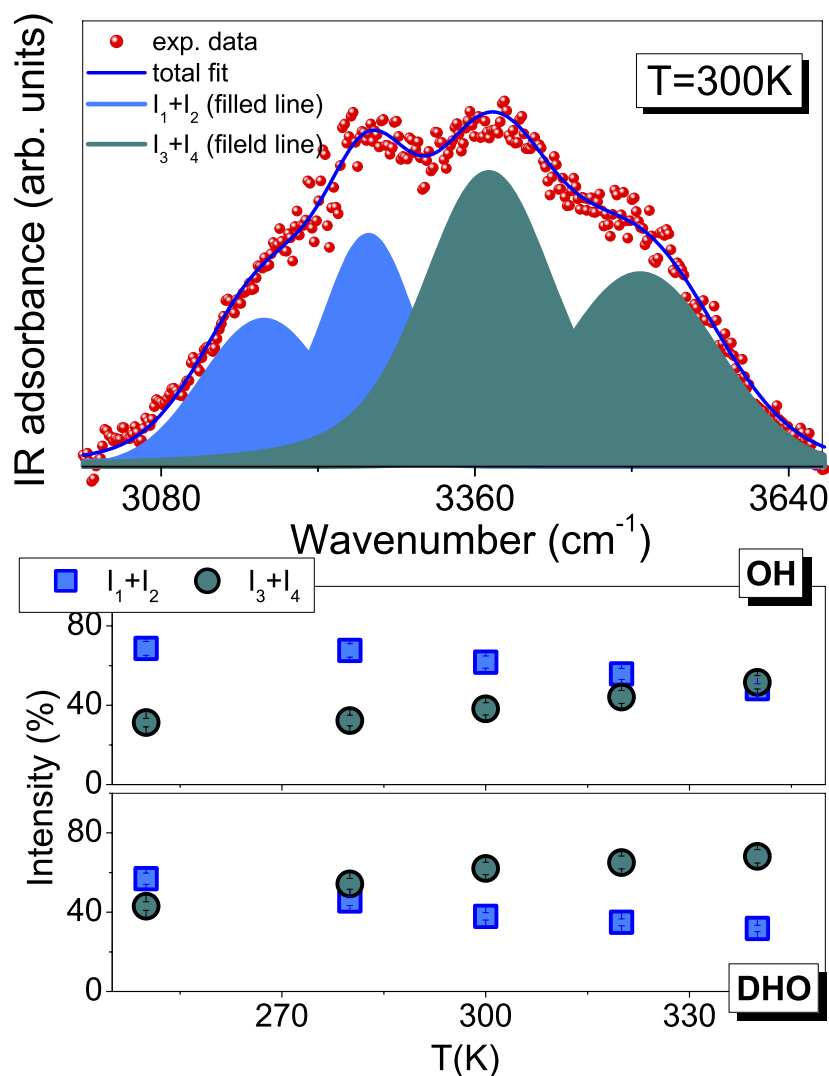


FIG. 8. (Panel at the top) Typical schematic of the fitting procedure results for DHO spectrum of β -CDPMA14 nanosponge hydrogel at $T = 300\text{ K}$. (Panel at the bottom) Percentage intensities $I_1 + I_2$ and $I_3 + I_4$ of the spectral contributions to the DHO and OH stretching band as a function of temperature, T , for β -CDPMA14 hydrogel.

not bulk-like water molecules becomes favoured with respect to the population of bulk-like water is significantly shifted to high temperature values (about $T = 340\text{ K}$) with respect to the DHO. This experimental evidence can be explained by taking into account that the water molecules more closely confined in the cavities of polymer preferably develop HB networks with connectivity less than four, even at low temperature, due to the proximity with the chemical groups of CDNS. Therefore, we can conclude that the analysis of the DHO spectra can provide direct information on the CDNS-water interaction during the confinement of water in the pores of polymer.

IV. CONCLUSION

The molecular connectivity and the extent of hydrogen-bonds patterns of water molecules confined in nanosponge hydrogels are here investigated as a function of temperature by using vibrational spectroscopy experiments. The system chosen for our study, namely, cyclodextrin nanosponge, is

a new promising class of cross-linked polymers that exhibit pronounced properties of sorption of water or water solutions that are recently widely investigated also for their practical and technological interest. However, CDNS represent also a good model system for the motivations of the present work, which aims to propose and test an experimental spectroscopic method useful for probing the structure and dynamics of confined water in nano-porous polymeric systems.

The combined analysis of the vibrational spectra of polymers hydrated with water and heavy water allows us to separate and selectively investigate the temperature-behaviour of the HOH bending mode of engaged water molecules and of the vibrational modes related to specific chemical groups of the polymer matrix involved in the HB interactions with water.

As main results, we find that the HOH bending mode of water in hydrogel exhibits, at temperatures below 270 K , a characteristic form quite different from the flattened profile typically observed for polycrystalline ice, giving a strong experimental evidence of a liquid-like behaviour of the H_2O molecules confined in the nano-cavities of polymer matrix.

Moreover, the changes in wavenumber position and intensity observed for HOH bending mode of water upon the increase of temperature indicate a characteristic destructuring effect on the hydrogen bond pattern of confined water molecules, induced by thermal motion. More interestingly, we find that the extent of this temperature-disruptive effect is triggered by the level of the cross-linking density of the nanosponge polymer through the key parameter, n . The rationale of these experimental findings could rely on the establishment of intra-molecular HB network involving the C=O groups of CDNS which are favoured (at $n = 6$) at the expense of the population of water molecules arranged in tetrahedral HB patterns and vice versa (at high values of n). This seems to confirm, in turn, the hypothesis that for $n = 6$, we observe an ideal balance between activated carboxylic groups and free hydroxyl functions onto the CD units, leading to the highest covalent interconnectivity in the polymer. All these results contribute to give a more clear picture of the molecular mechanism of water confinement in the pores of nanosponge hydrogel, whose understanding is a fundamental starting point for the modulation of the properties of gel phases, also in view of the design of stimuli-responsive CDNS. Actually, the different absorption capacity of nanosponges can be explained, at molecular level, by the competition between different factors, i.e., the cross-linking density of polymer matrix, the reduced dimensions of the pores of the CDNS, and the re-organisation of water confined in the nano-cavities of nanosponges in HB networks at different levels of connectivity. Interestingly, all the experimental results seem to suggest that the swelling phenomena can be efficiently regulated at molecular level through the molar ratio, n .

In perspective, the generality of the findings of this work opens the possibility to exploit the spectroscopic method here proposed as investigating tools for water-retaining soft materials.

ACKNOWLEDGMENTS

We would like to thank Dr. Marco Paolantoni for the useful and stimulating discussions.

- ¹R. Langer and J. P. Vacanti, *Science* **260**, 920 (1993).
- ²R. P. Lanza, R. S. Langer, and J. Vacanti, *Principles of Tissue Engineering*, 3rd ed. (Elsevier/Academic Press, Amsterdam, Boston, 2007).
- ³A. Atala, R. P. Lanza, J. A. Thomson, and R. M. Nerem, *Principles of Regenerative Medicine* (Academic Press, Burlington, MA, 2008).
- ⁴R. Langer, *Adv. Mater.* **21**, 3235 (2009).
- ⁵M. S. Shoichet, *Macromolecules* **43**, 581 (2010).
- ⁶G. Perale, F. Rossi, M. Santoro, P. Marchetti, A. Mele, F. Castiglione, E. Raffa, and M. Masi, *J. Biomed. Nanotechnol.* **7**(3), 476 (2011).
- ⁷M. Santoro, P. Marchetti, F. Rossi, G. Perale, F. Castiglione, A. Mele, and M. Masi, *J. Phys. Chem. B* **115**(11), 2503 (2011).
- ⁸G. M. Spinks, C. K. Lee, G. G. Wallace, S. I. Kim, and S. J. Kim, *Langmuir* **22**, 9375 (2006).
- ⁹A. A. De Angelis, D. Capitani, A. Segre, and V. Crescenzi, *Polym. Prep.* **42**, 45 (2001).
- ¹⁰F. Hua and M. Qian, *J. Mater. Sci.* **36**, 731 (2001).
- ¹¹F. Trotta, W. Tumiatti, R. Cavalli, O. Zerbinati, C. M. Roggero, and R. Vallero, WO patent 06/002814 (2006).
- ¹²F. Trotta and W. Tumiatti, WO patent 03/085002 (2003).
- ¹³F. Trotta, W. Tumiatti, R. Cavalli, C. M. Roggero, B. Mognetti, and G. Bertanico, WO patent 09/003656 (2009).
- ¹⁴L. Seglie, K. Martina, M. Devacchi, C. Roggero, F. Trotta, and V. Scariot, *Postharvest Biol. Technol.* **59**, 200 (2011).
- ¹⁵D. Li and M. Ma, *Clean Prod. Processes* **2**, 112 (2000).
- ¹⁶E. Memisoglu-Bilensoy, I. Vural, A. Bocho, J. M. Renoir, D. Duchene, and A. A. Hincal, *J. Controlled Release* **104**, 489 (2005).
- ¹⁷F. Trotta, M. Zanetti, and R. Cavalli, *Beilstein J. Org. Chem.* **8**, 2091 (2012).
- ¹⁸S. V. Chhajlwar, P. P. Pednekar, K. R. Jadhav, G. J. C. Gupta, and V. J. Kadam, *Expert Opin. Drug Delivery* **11**(1), 111 (2014).
- ¹⁹A. Mele, F. Castiglione, L. Malpezzi, F. Ganazzoli, G. Raffaini, F. Trotta, B. Rossi, A. Fontana, and G. Giunchi, *J. Inclusion Phenom. Macrocyclic Chem.* **69**, 403 (2011).
- ²⁰V. Crupi, D. Majolino, A. Mele, B. Rossi, F. Trotta, and V. Venuti, *Soft Matter* **9**, 6457 (2013).
- ²¹W. Liang, C. Yang, D. Zhou, H. Haneoka, M. Nishijima, G. Fukuhara, T. Mori, F. Castiglione, A. Mele, F. Caldera, F. Trotta, and Y. Inoue, *Chem. Commun.* **49**, 3510 (2013).
- ²²V. Crupi, A. Fontana, D. Majolino, A. Mele, L. Melone, C. Punta, B. Rossi, F. Rossi, F. Trotta, and V. Venuti, *J. Inclusion Phenom. Macrocyclic Chem.* **80**, 69 (2014).
- ²³F. Castiglione, V. Crupi, D. Majolino, A. Mele, L. Melone, W. Panzeri, C. Punta, B. Rossi, F. Trotta, and V. Venuti, *J. Inclusion Phenom. Macrocyclic Chem.* **80**, 77 (2014).
- ²⁴V. Crupi, D. Majolino, A. Mele, L. Melone, C. Punta, B. Rossi, F. Toraldo, F. Trotta, and V. Venuti, *Soft Matter* **10**, 2320 (2014).
- ²⁵M. Ferro, F. Castiglione, C. Punta, L. Melone, W. Panzeri, B. Rossi, F. Trotta, and A. Mele, *Beilstein J. Org. Chem.* **10**, 2715 (2014).
- ²⁶B. Rossi, S. Caponi, F. Castiglione, S. Corezzi, A. Fontana, M. Giarola, G. Mariotto, A. Mele, C. Petrillo, F. Trotta, and G. Viliani, *J. Phys. Chem. B* **116**(17), 5323 (2012).
- ²⁷F. Castiglione, V. Crupi, D. Majolino, A. Mele, B. Rossi, F. Trotta, and V. Venuti, *J. Phys. Chem. B* **116**(43), 13133 (2012).
- ²⁸F. Castiglione, V. Crupi, D. Majolino, A. Mele, B. Rossi, F. Trotta, and V. Venuti, *J. Phys. Chem. B* **116**(27), 7952 (2012).
- ²⁹V. Crupi, A. Fontana, M. Giarola, S. Longeville, D. Majolino, G. Mariotto, A. Mele, A. Paciaroni, B. Rossi, F. Trotta, and V. Venuti, *J. Phys. Chem. B* **118**(2), 624 (2014).
- ³⁰V. Crupi, A. Fontana, M. Giarola, D. Majolino, G. Mariotto, A. Mele, L. Melone, C. Punta, B. Rossi, F. Trotta, and V. Venuti, *J. Raman Spectrosc.* **44**(10), 1457 (2013).
- ³¹G. E. Walrafen, *Structure of Water and Aqueous Solutions*, edited by W. A. P. Luck (Verlag Chemie, Weinheim, Germany, 1974).
- ³²G. E. Walrafen, M. S. Hokmababi, and W. H. Yang, *J. Chem. Phys.* **85**, 6964 (1986).
- ³³G. D'Arrigo, G. Maisano, F. Mallamace, P. Migliardo, and F. Wanderlingh, *J. Chem. Phys.* **75**, 4264 (1981).
- ³⁴J. B. Brubach, A. Mermet, A. Filabozzi, A. Gerschel, and P. Roy, *J. Chem. Phys.* **122**, 184509 (2005).
- ³⁵M. Paolantoni, N. Faginas Iago, M. Albert, and A. Lagana, *J. Phys. Chem. A* **113**, 15100 (2009).
- ³⁶L. Liu, S. H. Chen, A. Faraone, C. W. Yen, and C. Y. Mou, *Phys. Rev. Lett.* **95**, 117802 (2005).
- ³⁷P. C. Shih, H. P. Lin, and C. Y. Mou, *Stud. Surf. Sci. Catal.* **146**, 557 (2003).
- ³⁸F. Mallamace, M. Broccio, C. Corsaro, A. Faraone, U. Wanderlingh, L. Liu, C. Y. Mou, and S. H. Chen, *J. Chem. Phys.* **124**, 161102 (2006).
- ³⁹M. F. Chaplin, *Structuring and behaviour of Water in Nanochannels Confined in Adsorption Phase Behaviour in Nanochannels Nanotubes*, edited by L. Dunne and G. Manos (Springer, 2010).
- ⁴⁰F. Mallamace, M. Broccio, C. Corsaro, A. Faraone, D. Majolino, V. Venuti, L. Liu, C. Y. Mou, and S. H. Chen, *Proc. Natl. Acad. Sci. U. S. A.* **104**, 424 (2007).
- ⁴¹F. D'Amico, M. Saito, F. Bencivenga, M. Marsi, A. Gessini, G. Camisasca, E. Principi, R. Cucini, S. DiFonzo, and A. Battistoni, *Nucl. Instrum. Methods Phys. Res., Sect. A* **703**, 33 (2013).
- ⁴²V. Crupi, D. Majolino, A. Paciaroni, B. Rossi, R. Stancanelli, V. Venuti, and G. Viliani, *J. Raman Spectrosc.* **41**(7), 764 (2010).
- ⁴³C. Cannavà, V. Crupi, P. Ficarra, M. Guardo, D. Majolino, R. Stancanelli, and V. Venuti, *Vib. Spectrosc.* **48**, 172 (2008).
- ⁴⁴F. Castiglione, V. Crupi, D. Majolino, A. Mele, B. Rossi, F. Trotta, and V. Venuti, *J. Raman Spectrosc.* **44**(10), 1463 (2013).
- ⁴⁵A. Millo, Y. Raichlin, and A. Katzir, *Appl. Spectrosc.* **59**, 460 (2005).
- ⁴⁶V. Crupi, D. Majolino, P. Migliardo, V. Venuti, and M. C. Bellissent-Funel, *Mol. Phys.* **101**, 3323 (2003).
- ⁴⁷R. Bergman and J. Swanson, *Nature* **403**, 283 (2000).

- ⁴⁸V. Crupi, F. Longo, D. Majolino, and V. Venuti, *J. Chem. Phys.* **123**, 154702 (2005).
- ⁴⁹B. Rossi, A. Fontana, M. Giarola, G. Mariotto, A. Mele, C. Punta, L. Melone, F. Toraldo, and F. Trotta, *J. Non-Cryst. Solids* **401**, 73 (2014).
- ⁵⁰G. Bellavia, L. Paccou, S. Achir, Y. Guinet, J. Siepmann, and A. Hédoux, *Food Biophys.* **8**, 170 (2013).
- ⁵¹J. R. Scherer, M. K. Go, and S. J. Kint, *J. Phys. Chem.* **78**, 1304 (1974).
- ⁵²T. T. Wall and D. F. J. Hornig, *J. Chem. Phys.* **43**, 2079 (1965).
- ⁵³W. F. Murphy and H. J. J. Bernstein, *J. Phys. Chem.* **76**, 1147 (1972).
- ⁵⁴A. Hédoux, Y. Guinet, and L. J. Paccou, *J. Phys. Chem. B* **115**, 6740 (2011).
- ⁵⁵G. D'Arrigo, G. Maisano, F. Mallamace, P. Migliardo, and F. J. Wanderlingh, *J. Chem. Phys.* **75**, 4264 (1981).
- ⁵⁶G. E. J. Walrafen, *J. Chem. Phys.* **47**, 114 (1967).
- ⁵⁷N. Goldman and R. J. Saykally, *J. Chem. Phys.* **120**, 4777 (2004).
- ⁵⁸P. A. Giguère, *J. Chem. Phys.* **87**, 4835 (1987).
- ⁵⁹M. Freda, A. Piluso, A. Santucci, and P. Sassi, *Appl. Spectrosc.* **59**, 1155 (2006).
- ⁶⁰D. A. Schmidt and K. Miki, *J. Phys. Chem. A* **111**, 10119 (2007).